Original Article

IN SILICO PROBING OF ANTI-ARTHRITIC POTENTIAL OF TRADITIONALLY FERMENTED AYURVEDIC POLYHERBAL PRODUCT BALARISHTA REVEALS LUPEOL AND DESULPHOSINIGRIN AS EFFICIENT INTERACTING COMPONENTS WITH UREC

ANNADURAI VINOTHKANNA[1], PARAMASIVAN MANIVANNAN[2], GANGATHARAN MURALITHARAN[2], SOUNDARAPANDIAN SEKAR[1]*

[1]Department of Industrial Biotechnology, Bharathidasan University, Tiruchirappalli, Tamilnadu, India, [2]Department of Microbiology, Bharathidasan University, Tiruchirappalli, Tamilnadu, India.
Email: sekarbiotech@yahoo.com

ABSTRACT

Objective: To assess the anti-arthritic properties of *Balarishta*, an Ayurvedic fermented poly herbal product used to combat the immunological disorder, Rheumatoid Arthritis which is an autoimmune disease triggered by *Proteus* urinary tract infection through *in silico* analysis and assay of antimicrobial activity.

Methods: Antibacterial activity of *Balarishta* against *Proteus mirabilis* was assessed. Phytochemical analysis was performed by Gas Chromatography-Mass Spectroscopy. Urease interaction proteins were homology modeled based on template constraints and physicochemical parameters and stereo chemical nature of the proteins were analyzed. Rigid and flexible docking was done to study the hydrogen bond interaction patterns between active ingredients of *Balarishta* and urease interaction proteins.

Results: In *Balarishta,* 42 bioactive metabolites were identified by Gas Chromatography-Mass Spectroscopy analysis*.* These metabolites were checked for strong binding affinities against urease subunits and urease accessory proteins of *Proteus mirabilis in silico.* ureC subunit exhibited high binding to the compound desulphosinigrin (-10.5217 Kcal/mol) followed by lupeol (-10.0308 Kcal/mol) with conserved residue interaction ranging from amino acid residues 308 – 327. Further, lupeol when bound to ureC had 4 hydrogen bonds as compared to desulphosinigrin with 6 hydrogen bonds. Free energy calculations based on flexible docking showed that lupeol had significant binding affinity for ureC with -9.2 Kcal/mol rather than -6.0 Kcal/mol for desulphosinigrin. Both binding has residue conservation - Cys 319, His 320 and His 321. The results corroborated with *in vitro* antibacterial activity.

Conclusion: It is proposed that *Balarishta* would be efficient in arresting Rheumatoid Arthritis complicated urinary tract infections.

Keywords: Ayurveda, *Balarishta*, Polyherbal fermentation, Urinary Tract Infection, Rheumatoid Arthritis, *Proteus mirabilis*, Urease proteins, Computational Pharmacology, Molecular docking.

INTRODUCTION

Arishta and *Asava* are self-generated polyherbal fermented medicines of traditional Ayurvedic system. *Arishta* are made with decoctions of herbs in boiling water while *Asava* are prepared by directly using fresh herbal juices. *Balarishta* is prepared by using 11 herbal ingredients and the main herb is bala (*Sida rhombifolia* L.*)* [1]. *Balarishta* has been traditionally used to treat Rheumatoid Arthiritis (RA) by Ayurvedic practitioners [2]. However, there is no research on validation of the therapeutic property.

RA have been categorized by infectious pathogens and have been demarcated into six stages.[3]namely, first stage of infection by *Proteus* group of pathogens in which Subclinical UTI's is caused by *Proteus* sp. That result in asymptomatic bacteriuria[4, 5, 6]. Notably, *Escherichia coli* do not cross react with type XI collagen as they lack urease production. *E. coli* is responsible for 70 – 80% of urinary tract infection. Nevertheless, *Proteus* elicits RA like symptoms by producing antibacterial antibodies intended in causing RA [7]. Second stage of complication can be possibly attributed to antibodies production against *Proteus* urease and haemolysin in local lymph nodes [4]. Thirdly, cytotoxicity targeting hyaline cartilage and HLA-DR1/4 positive chondrocytes mimicks the mode of action of collagen XI resulting in an enormous accumulation of autoantibodies against joint tissues that are rich in collagen [8]. The disease progressively damages synovial tissues by macrophage infiltration and lymphocyte accumulation leading to release of cytokines and chemokines [4]. Stage five comprises of collateral damage through secondary cytotoxicity and moreover there will be no self / non self recognition as *Proteus* urease mimicking results in diminished activity of TNF-α [4]. Repetitive progress in *Proteus*

infection causes recurring inflammation, joint damage, deformities and ultimately RA. So, *P. mirabilis* and its urease are the cause for the manifestation of RA. Urease (EC 3.5.1.5) is a nickel containing enzyme having its role in nitrogen circulation and was the first enzyme that has been crystallized [3]. *P. mirabilis* urease has a molecular weight of about 212 to 250 kDa and is composed of three subunit polypeptides, ureA, ureB, and ureC, within the ratio of 2:2:1, respectively [9]. Other subunits involved in the present study include ureD, ureE, ureF, ureG, ureR, Hns, PMI1793 and pqrA which are urease accessory proteins**.** Hence, the antimicrobial activity of *Balarishta* against *P. mirabilis* was assessed, its phytochemical profile by Gas Chromatography-Mass Spectroscopy (GC-MS) analysis was performed and finally the ability of constituent components to bind with urease subunits was performed *in silico* in order to validate the ability of *Balarishta* in treating RA.

MATERIALS AND METHODS

Sampling

The sample was collected from the manufacturing unit of M/S. Astanga Ayurvedics (P) Ltd, Tiruchirappalli, Tamilnadu, India.

Antibacterial activity of *Balarishta* against *Proteus mirabilis*

Urinary as well as enteropathogenic culture namely, *Proteus mirabilis* MTCC425 was obtained from Microbial Type Culture Collection, Chandigarh. Air Dried Mueller-Hinton Agar plates (MHA) were prepared and the pathogenic organism was inoculated as a lawn using sterile swabs. After inoculation, the UTI discs (Himedia UTI5 and UTI11) which contain Ampicilin (10μg), Ciprofloxacin (5μg), Co-Trimoxazole (25μg), Amoxyclav (30μg), Nitrofurantoin

(300μg), Norfloxacin (10 μg), Fosfomycin (200 μg), Amikacin (30 μg), Gentamycin (10μg), and Ceftriaxone (30μg) that are purchased from HI-Media, Mumbai, were placed in the centre of MHA plates. After 16-18 hours of incubation, the diameter of zone of inhibition were measured and recorded. Similarly, *Balarishta* sample was also tested using the same method. The *Balarishta* sample was placed in a hot air oven at 75ºC for 10 min. to evaporate ethanol in the sample. Then 100 μl of the sample was tested by well and disc similar to Kirby Bauer method [10]. Ten percent of ethanol (samples contain 10% of ethanol at the maximum) loaded in disc and well are treated as controls. Experiments were performed in triplicates and reported as mean ± standard deviation. The relative percentage inhibition of the test sample (*Balarishta)* was calculated using the following formula, 100- (X-Y) / (Z-Y) where X = Total area of inhibition of the test sample, Y = Total area of inhibition of the solvent, Z = Total area of inhibition of the standard antibiotic (The antibiotic exhibiting maximum zone of inhibition). The total area of inhibition was calculated by using the formula, πr^2 where, r = Radius of zone of inhibition [11].

GC-MS analysis

Balarishta sample was concentrated and the maximum amount of water removed using evaporation in the hot air oven at 80°C for 24-48 hours before GC-MS (PerkinElmer Clarus 500) analysis. Fifteen ml of sample was frozen using deep freezer for one day at - 20°C and then, the frozen sample was concentrated with the help of vacuum evaporator at – 80°C. The frozen dried sample was dissolved in 10 ml of HPLC grade methanol and GC-MS analysis was performed. One micro liter of sample was injected (split ratio 1:8) into the GC-MS system on a 30-m capillary column with a film thickness of 0.25 μm (30m x 0.25 mm i. d. coated with 5% Phenyl 95%dimethylpolysiloxane) using the two types of oven temperature were followed to get maximum responses. Helium was the carrier gas with flow rate of 1 ml/min. Injection temperature was 280°C. Initial oven temperature of 50°C at 10°C/min to 150°C at 8°C/min to 280°C (10 min*) and then 60°C at 8°C/min to 200°C at 10°C/min to 300°C(5 min*) were used (Scan type: full scan mode, Scan range: 40-450 daltons). The peaks are matched with phytochemistry Library: NIST (The National Institute of Standards and Technology) MS search library version 2.0.

Homology modeling

Confidence interval map of urease accessory proteins was analyzed from STRING database [12] and availability for authentic structures in Protein Data bank was checked comparatively in NCBI Entrez, PDB and SWISSPROT databases. The protein sequences for urease interaction proteins were retrieved from the STRING database. Suitable templates for the above mentioned proteins were selected using the homology detection and structure prediction by HMM-HMM comparison in [13] the templates chosen had an e value <1.0 and similarity >90%.

Theoretical Isoelectric point (pI), molecular weight, number of positively and negatively charged residues, extinction coefficient, Instability Index, Aliphatic Index and Grand average hydropathicity (GRAVY) were computed using the Expasy's protparam server [14]. The SOSUI Server [15] was used to characterize whether the protein is soluble or transmembrane in nature. Disulphide linkages were found by DISULFIND Server.

Secondary structure was predicted using PSIPRED Server [16]. The modeling of the three dimensional structure of the protein was performed by MODELLER9V12 [17]. The constructed models were energy minimized by CHIMERA [18]. The overall stereochemical properties of the proteins were analyzed in the RAMPAGE Server [19]. The three dimensional structures were further verified by VERIFY3D [20]. RMS-Z score for bond angles of modeled protein structure was estimated by QMEAN Server [21]. The models are viewed in PYMOL [22]. Ligand binding site and pockets were predicted by CASTp Server [23] and QSITE FINDER [24].

Preparation of ligands

The ligand used for the study was downloaded from Pubchem project database [25] and Chemspider database [26].

The conversion of SMILES to PDB files was done for generation of 2D structure of *Balarishta* active ingredients. RMSD based energy minimization was performed in *vacou* to give a first optimization of the rough structure using VEGA ZZ [27]. Hydrogens were initially added to receptor molecule, AMBER and gasteiger charges were added to fix unusual bonds in the 3D structure which utilizes CHARMM force field parameters. The 2D model was optimized and energy minimized using clean geometry option in ArgusLab 4.0. [28].

Docking perspectives

Docking between urease interaction proteins and active ingredients of *Balarishta* was performed by Patchdock server [29]. Energy minimization was performed before and after docking using GROMOS96 version of SWISS-PDB Viewer [30]. Hydrogen bond interactions were assessed by Discovery studio 3.5. [31] and molegro virtual docker [32]. Docked view of the complexes was visualized using Pymol. Flexible docking with AUTODOCK VINA involving whole protein as the receptor molecule was performed and the binding sites were automatically detected [33].

RESULTS AND DISCUSSION

Antibacterial activity

Antibacterial activity of *Balarishta* against *P. mirabilis* were assessed in comparison with standard antibiotics in clinically recommended dosage (Table 1). It indicates that Ciprofloxacin is most effective even at the level of 5μg/disc. Activity of *Balarishta* is comparable in both well method and disc method and it is close to the antibiotic Nitrofurantoin (300μg). It implies that *Balarishta* also have modest antibacterial property against *Proteus mirabilis.*

However, it was tested at a concentration of 100 μl of *Arishta* sample per disc where the *Balarishta* is heterogenous with polyherbal drugs, ethanol and other ingredients. But the activity of 100 μl of *Balarishta* could match with the pure antibiotic Nitrofurantoin at 300μg. However, gentamycin (10μg) is most effective against *P. mirabilis* MTCC425 with the highest zone of inhibition. Relative percentage inhibition of the test sample (*Balarishta,* 100 μl/disc*)* when compared with gentamycin is 10.23% only.

Table 1: Antibacterial activity of *Balarishta* in comparison with reference antibiotics (in hexa-disc) against *Proteus mirabilis* MTCC425

Antibiotics/ *Balarishta* (concentration)	*Proteus mirabilis* MTCC425 (Diameter of zone of inhibition in mm)
Ampicilin (10μg)	25±1.00
Ciprofloxacin (5μg)	37±0.50
Co-Trimoxazole (25μg)	26±0.60
Amoxyclav (30μg)	25±0.53
Nitrofurantoin (300μg)	13±0.50
Norfloxacin (10μg)	36±1.00
Fosfomycin (200μg)	33±0.30
Amikacin (30μg)	26±0.70
Gentamycin (10μg)	39±0.90
Ceftriaxone (30μg)	0±0.00
Balarishta (100 μl/well) Zone of inhibition in well method	12±0.20
Balarishta (100 μl/disc) Zone of inhibition in disc method	12.5±0.50

(Values are expressed as mean ± standard deviation of the triplicates)

GC-MS analysis

Phytochemical analysis of *Balarishta* by GC-MS using two different temperature programs (Figure 1) indicates the presence of an array of phytochemicals (Table 2). There are 42 compounds as per this analysis. These compounds were subjected to docking analysis.
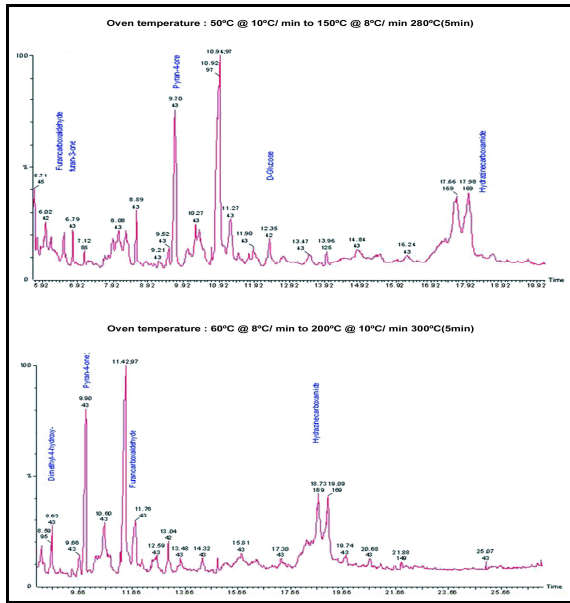
Fig. 1: GC-MS spectra of *Balarishta* performed in two different oven temperature programs.

subunit, ureC, is highly conserved for every urease studied so far and has been regarded as active site residues for ureC [9].
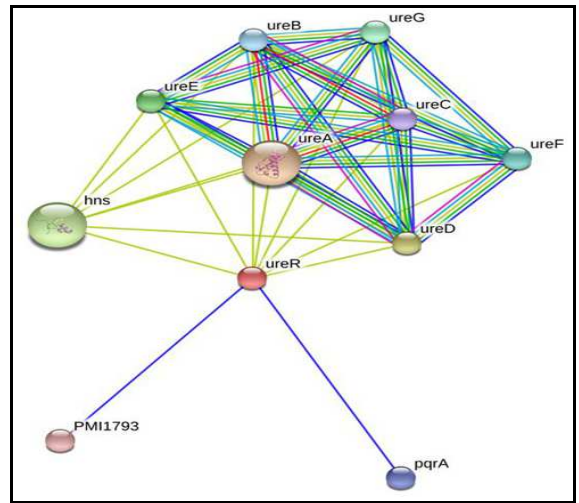

Fig. 2: Interaction network of urease interaction proteins.

Homology modeling

Figure 2 depicts urease accessory interaction proteins retrieved from STRING database. Urease accessory interaction proteins hns, pqrA, PMI1793, ureA, ureB, ureC, ureD, ureE, ureF, ureG and ureR were modeled using MODELLER 9V12 and was found that out of 11 proteins five were found stable (Table 3). The stable proteins include ureA, ureB, ureC, ureE and ureG. All the proteins were found to be soluble in nature. Stability plays a pivotal role in deciphering binding affinities, hence stereochemical analysis and RMS-Z score of proteins were considered as efficient for categorizing conformationally stable proteins and ureC was identified as stable from the Ramachandran plot analysis (Figure 3b & 3c). The protein ureC had high quality as evident from the number of residues in the favourable region (537). Moreover least number of residues in the outlier region (3) affirms the above fact. Low RMS-Z score of -4.95 showed clearly that ureC as an efficient protein for further studies. Table 3 depicts the physicochemical parameters of the modeled proteins and the qualitative ureC are indicated in red. UreC as compared to other proteins has significantly high aliphatic index of 92.72 and low instability index 36.12 establishing that ureC as a stable component when taken in to modeling perspective and aliphatic index renders the protein to be of more binding affinity patterns. Nevertheless, high amount of positive (66) and negatively charged residues (47) also confirm that ureC to be an effective interacting partner to other ligands. Figure 3a) illustrates the homology modeled structure of ureC with alpha helix pictorially shown in yellow, Beta strand in red and coils in green colour. Furthermore, Figure 3d) depicts secondary structure patterns of the modeled protein. Analysis of pockets and clefts in computed surface topology of proteins showed high number of pockets (85) with a surface area 5634.6 and volume 13806 for ureC using solvent probe of radius 1.4 angstrom (Table 4). Further, DISULFIND results affirmed the disulfide bridges with highest (9) cysteine residues for ureC (Table 4). Table 5 depicts energy minimization values and ureC has a high energy of -9469.724 KJ/mol, Although, ureR has a high value than ureC with -9675.076 KJ/mol, due to its low stability which is not taken in to account in the present study. Similar study by Paramasivan et al involves homology modeling of urease accessory interaction proteins of *Helicobacter Pylori* J 99 and predicting an efficient interruption of interaction by *Vigna radiata* defensins showed that ureH and ureI are efficiently abated by VrD1 and VrD2 defensins [34].

Docking perspectives

Experimental evidence showed that in *Proteus mirabilis* urease, residues 308 to 327 (TVDEHLDMLMVCHHLDPSIP) in large urease
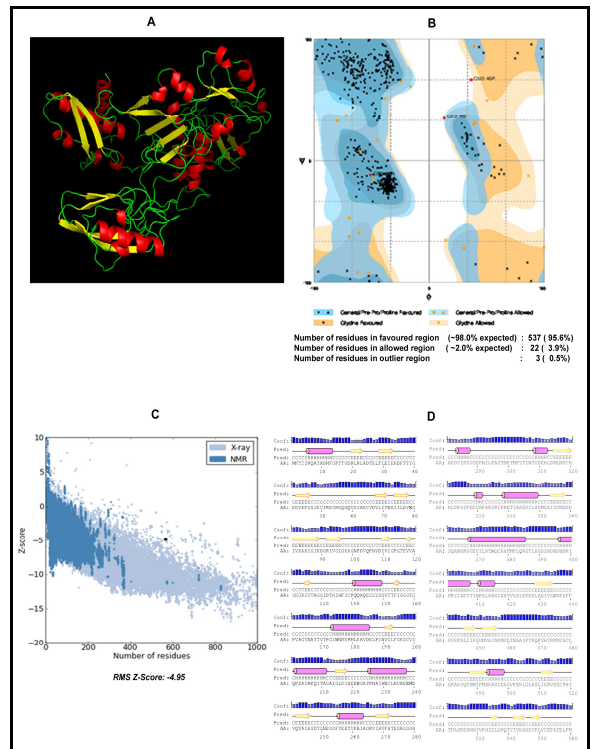

Fig. 3: A) Homology modeled structure of ureC with alpha helix shown in yellow, beta sheet in red and coils in green color. B) stereochemical nature of the protein ureC. C) Quality of protein ureC as predicted by RMSZ score. D) Secondary structure of ureC.

Among the active site residues, ASAVIEW was used to depict the nature of amino acid residues and was demarcated in to positive charged, negatively charged, polar uncharged, Cysteine residues and hydrophobic nature. Analysis revealed that the active site residues are hydrophobic rich but are conformationally stable. Figure 4 (a, b, c and d) shows the one dimensional and three dimensional images of Desulphosinigrin (DSS) and lupeol that were found to interact prominently with ureC. Lupeol is a pentacyclic triterpene and was found to be anti inflammatory [35] anti arthritic [36], anti urolithiatic [37] and hepatoprotective in rats [38].

Table 2: Chemical compounds identified in *Balarishta* by GC-MS analysis using two different oven temperature programs.

S. No.	Retention time Temp. 1	Temp. 2	Name of the chemical compounds
1.	6.79	6.56	2,4-Dihydroxy-2,5-dimethyl-3(2H)-furan-3-one
2.	8.29	8.63	2,5-Dimethyl-4-hydroxy-3(2H)-furanone
3.	10.95	11.41	2-Furancarboxaldehyde, 5-(hydroxymethyl)-
4.	6.53	6.27	2-Furancarboxaldehyde, 5-methyl-
5.	4.82	4.34	2-Furanmethanol
6.	7.11	6.91	2H-Pyran-2,6(3H)-dione
7	6.18	5.44	2-Propanone, 1,3-dihydroxy-
8.	9.69	9.90	4H-Pyran-4-one, 2,3-dihydro-3,5-dihydroxy-6-methyl-
9.	6.02	5.69	6-Oxa-bicyclo[3.1.0]hexan-3-one
10.	-	12.03	α -D-Glucopyranose, 4-O- α -D-galactopyranosyl-
11.	13.48	-	α -D-Glucopyranoside, O- α -D-glucopyranosyl-(1. fwdarw.3)- α -D-fructofuranosyl
12.	18.67	-	Desulphosinigrin
13.	12.35	13.04	D-Glucose, 4-O- α -D-glucopyranosyl-
14.	-	15.80	d-Glycero-d-ido-heptose
15.	-	5.87	DL-Arabinose
16.	4.53	4.15	Furfural
17.	-	4.54	Tetrahydropyrrole-3-amino-2,5-dione
18.	13.96	14.91	Uric acid
19.	17.98	18.73	Hydrazinecarboxamide, 2-(2-methylcyclohexylidene)-
20.	-	4.01	1,2-Epoxy-3-propyl acetate
21.	4.62	-	1H-Imidazole-4-ethanamine, N,5-dimethyl-
22.	-	10.27	2(3H)-Furanone, dihydro-4-hydroxy-
23	3.50	3.15	2,2'-Bioxirane, (R*,R*)-(ñ)-
.24.	3.93	3.48	2,3-Butanediol
25.	-	6.64	2-Deoxy-D-galactose
26.	7.21	-	2-Formyl-9-[α -d-ribofuranosyl]hypoxanthine
27.	5.69	-	(s) 2-Hydroxypropanoic acid
28.	-	2.41	2-Propanone, 1-hydroxy-
29.	9.51		2-Propanamine, N-methyl-N-nitroso-
30.	3.39	-	2-Propenoic acid, ethenyl ester
31.	5.27	-	4-Aminoisoxazolidin-3-one
32.	11.25	11.20	6-Acetyl- α -d-mannose
33.	-	2.90	Acetic acid, 1-methylethyl ester
34.	4.09	-	Carbonocyanidic acid, ethyl ester
35.	-	21.88	Dibutyl phthalate
36.	3.22	-	Glycerin
37.	10.03	-	Imidazole, 2-amino-5-[(2-carboxy)vinyl]-
38.	-	6.33	*Iso*-sorbide Dinitrate
39.	29.62	-	Lupeol
40.	-	2.62	Oxirane, 2,3-dimethyl-, trans-
41.	4.33	-	Pentylamine, N-isobutyl-N-nitroso-
42.	-	5.14	R-(-)-1,2-propanediol

Table 3: Physicochemical parameters of urease and its accessory interaction proteins

Protein	AA Length	MW (kda)	Theoretical pI	-ve charged residues (Asp + Glu)	+ve charged residues (Arg + Lys)	Extinction coefficients	Instability index	Aliphatic index	Grand average of hydropathicity (GRAVY)
Hns	134	15249.1	5.03	27	22	9970	52.05	85.30	-0.788
PMI1793	261	30036.4	7.70	31	32	36690	44.10	84.44	-0.333
pqrA	122	14308.4	9.48	15	21	15595	46.33	73.61	-0.600
ureA	100	10912.8	5.41	14	12	1615	37.86	104.30	0.102
ureB	108	12053.8	9.39	13	16	4470	39.93	80.37	-0.394
ureC	567	60927.0	5.44	66	47	50350	36.12	92.72	0.016
ureD	274	31008.8	6.31	27	24	53650	42.86	87.55	-0.112
ureE	161	17887.2	6.03	23	17	13075	31.44	88.39	-0.406
ureF	222	24992.7	5.41	24	19	51700	48.61	95.41	-0.032
ureG	205	22300.7	4.96	30	22	9065	23.26	103.71	-0.019
ureR	293	33415.4	8.15	24	26	23755	40.53	91.16	-0.125

Atomic contact energy values for lupeol - ureC was found to be -224.86 Kcal/mol, however for DSS- ureC it was -236.53 Kcal/mol. Docking with a grid resolution of 0.4 A⁰ showed that lupeol had a docking energy value of -10.0308 Kcal/mol with grid parameter value of X, Y, Z = 22.00, 34.25, 25.00 whereas, DSS at the same resolution with grid parameter 20.00, 22.75, 25.00 showed an increased value of energy ie., -10.5217 Kcal/mol. This binding affinity indicated large focused interaction between ureC and desulphosigrin compared to lupeol. Comparative analysis of Receptor ligand interactions depicts that lupeol with ureC had hydrogen bond interactions having Asn307, Thr308 and Glu311 as core interacting residues and DSS had Leu 316, Cys 319, His 320 and His321 as the pivotal residues at the interface. Figure 5 (a, b, c, d and e) depicts the hydrogen bond interactions between docked complexes of ureC with DSS and lupeol. The results indicated that lupeol has lesser binding affinity than DSS. This may be due to the fact that the latter has competitive efficacy with the lupeol. Moreover, this report is of its kind in suggesting a therapeutic notion

for DSS. The compound had been earlier described as a compound of aggravating agent for colon cancer in which it promoted the growth of HCT-116 (colon) and NCI H460 (lung) human cancer cells as evident from MTT assay at higher concentrations, wherein, μg/ml concentrations doubled the growth of HCT-116 colon cancer cells and for NCI H460 human lung cancer cells, DSS at 60μg/ml showed an increase in the cell number by 20% [39]. The above literature could be the only authentic citation that DSS has biological activity. Moreover, any component at a higher concentration may be deleterious. Hence, in the years to come we suggest that DSS could be a provocative agent in UTI therapeutics in a concentration dependent manner.

Antioxidant potentials of lupeol have been a largely studied arena in the case of hepatotoxicity [38] Arbitrarily, DSS acting as anti-UTI pharmaceuticals could invoke major clinical side effects, Hence we hypothesize that upon reduced concentrations DSS can have profound implications in treatment of UTI's. On the contrary, significant hepatoprotectivity by lupeol has its major role in lipid peroxidation wherein, peroxyl radicals scavenging is the main modality of anti oxidant property of lupeol [38], DSS doesn't have activity on lipid peroxidation at 250g/ml [39]. Binding energy values from flexible docking by AUTODOCK VINA showed that lupeol has an increased free energy of -9.2 Kcal/mol when compared to DSS which has -6.0 Kcal/mol (Figure. 6).

Table 4: Pockets and cysteine residues in the modeled proteins

Name of the protein	Pocket	Area	Volume	Cysteine residues
hns	14	127.6	178.2	-
PMI1793	48	651.8	1067.5	4
pqrA	19	318.5	787.1	2
ureA	17	263.1	370.6	2
ureB	21	97.9	197.8	-
ureC	85	5634.6	13806	9
ureD	50	652.1	836.1	5
ureE	22	883.6	2444	3
ureF	37	260	351.4	4
ureG	33	222.5	310.8	2
ureR	54	1346.3	1735.3	6

Table 5: Energy minimization values obtained for modeled proteins.

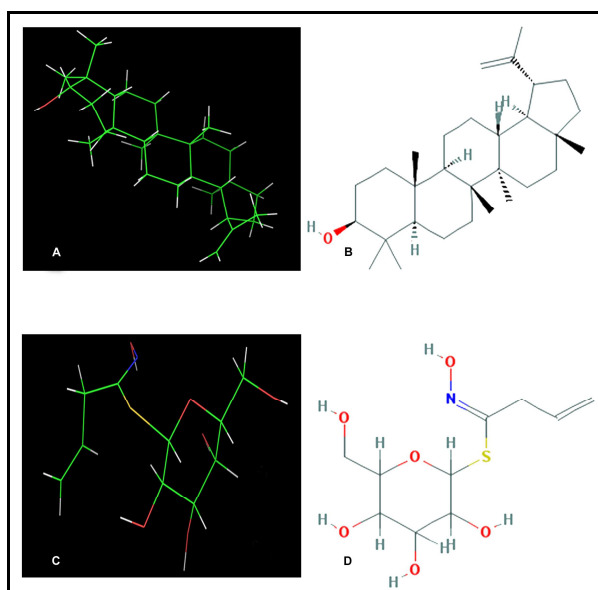| Name of the protein	Energy Minimization (KJ/mol)
hns	-4118.994
pqrA	-5487.629
PMI1793	15642.018
ureA	-3354.621
ureB	-2992.171
ureC	-9469.724
ureD	-6662.179
ureE	-4105.193
ureF	-5408.979
ureG	-5302.262
ureR	-9675.076

Fig. 4: A) and B) Three dimensional and one dimensional views of Desulphosinigrin respectively. C) and D) Three dimensional and one dimensional views of lupeol respectively.
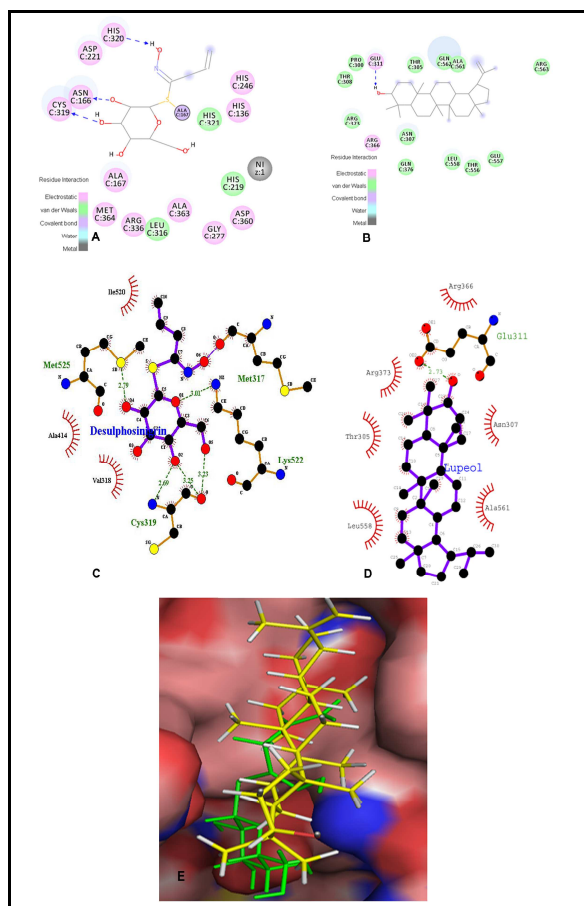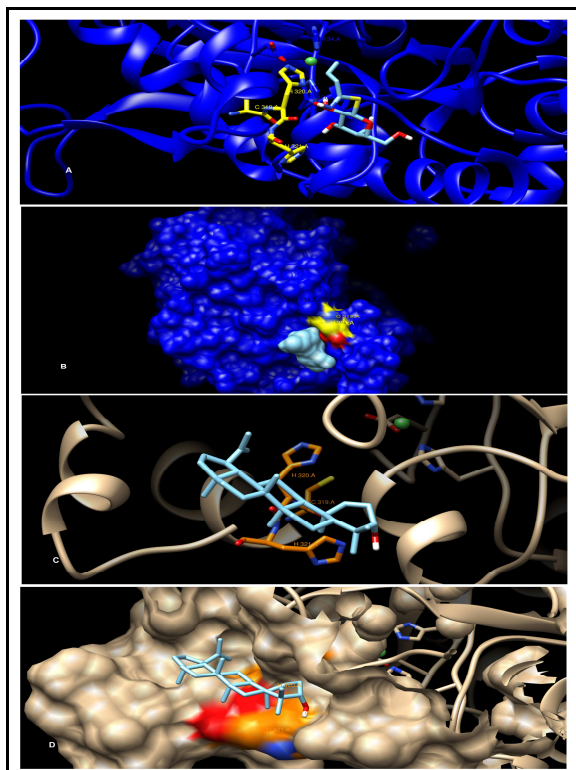

Fig. 5: A) Hydrogen bond interactions between desulphosinigrin and ureC. B) Hydrogen bond interactions between lupeol and ureC. C) Hydrogen bond interactions between of desulphosinigrin and ureC based on Ligplot. D) Hydrogen bond interactions between of lupeol and ureC based on Ligplot. E) Three dimensional views of interactions among ureC, desulphosinigrin (Green) and lupeol (Yellow).

Fig. 6: A) and B) Flexible docking results for desulphosinigrin. C) and D) Flexible docking results for lupeol

Further, Cys319, His320, and Ala167 contribute to catalysis of urea and was affirmed based on molecular dynamics simulations [40]. Dinickel binding on comparison with hydrogen bonding have been emancipated earlier that urease inhibitors are mostly conserved in structural conformation based on the binding motif that flaps the prominent orientation of the protein. To the core, nickel binding by tetrahedral coordination have been largely attributed for strong urease inhibition by urease inhibitors like diamidophosphate and I3A [40]. Future directions of research will be thrusted upon dinickel binding to lupeol. Therefore, there is every possibility of competitive inhibition of DSS activity by lupeol. Furthermore, abatement of RA by *Balarishta* has been traditionally documented in Ayurveda, a deep insight in to its molecular dissection of activity particularly with reference to UTI is still lacking. The present study would abridge the above gap and enhance insights in to antimicrobial properties of *Balarishta* and will have prominent impact in the field of complimentary therapies and alternative medicine.

CONCLUSIONS

UTI complicating RA has been regarded as a medical menace. Urease and its accessory interaction proteins are key virulent factors causing the infection. The present study addresses the issue by antibacterial activity assay against the causative agent, *P. mirabilis* and assessing the phytochemical components by GC-MS analysis. Further computational studies pertaining to homology modeling and docking of the phytochemicals were performed. DSS and lupeol were found to interact efficiently with ureC suggesting its role in therapeutic perspectives. Here, Hydrogen bond interactions rather than dinickel binding showed significant interactions. We further hypothesize that lupeol competitively binds to ureC in eliciting anti oxidant activities through lipid peroxidation. Hence, it is confirmative that lupeol apart from dinickel binding can elicit a protective response based on hydrogen bond affinities.

CONFLICT OF INTEREST

We declare that we have no conflict of interest.

REFERENCES

1. Sekar S, Mariappan S. Traditionally fermented biomedicines, *arishtas* and *asavas*, from Ayurveda. Indian J Tradit Knowl 2008;7:548-56.
2. Sekar S, Mariappan S. Fermented Medicines of Ayurveda: A Treatise. Germany; LAMBERT Academic Publishing (LAP); 2010.
3. Mobley HLT, Island MD, Hausinger RP. Molecular biology of microbial ureases. Microbiol Rev 1995;59:451-80.
4. Ebringer A, Rashid T. Rheumatoid arthritis is caused by a *Proteus* urinary tract infection. APMIS 2013;122:363–8.
5. Lawson AA, Maclean N. Renal disease and drug therapy in rheumatoid arthritis. Ann Rheum Dis 1966;25:441-9.
6. Tishler M, Caspi D, Aimog Y, Segal R, Yaron M. Increased incidence of urinary tract infection in patients with rheumatoid arthritis and secondary Sjogren's syndrome. Ann Rheum Dis 1992;51:601-6.
7. Rashid T, Ebringer A. Rheumatoid arthritis is caused by asymptomatic *Proteus* urinary tract infections. In: Nikibakhsh AA editors. Clinical management of complicated urinary tract infection. Rijeka In Tech; 2011. p. 171-80.
8. Wilson C, Rashid T, Tiwana H, Beyan H, Hughes L, Bansal S. Cytotoxicity responses to peptide antigens in rheumatoid arthritis and ankylosing spondylitis. J Rheum 2003;30:972-8.
9. Sriwanthana B, Mobley HLT. *Proteus mirabilis* Urease: Histidine 320 of ureC is essential for urea hydrolysis and nickel ion binding within the native enzyme. Infect Immun 1993;61:2570-7.
10. Bauer AW, Kirby WMM, Sherris JC, Turck M. Antibiotic susceptibility testing by a single high content disk method. Amer J Clin Pathol 1966;45:492-6.
11. Naz R, Bano A. Antimicrobial potential of *Ricinus communis* leaf extracts in different solvents against pathogenic bacterial and fungal strains. Asian Pac J Trop Biomed 2012;2:944-7.
12. Franceschini. STRING database 9.1. Available: URL: http://string-db.org/.
13. Homology detection & structure prediction by HMM-HMM comparison. (2014). Available: URL: http://toolkit.tuebingen.mpg.de/hhpred. [Last accessed 11th Apr 2014].
14. Expasy's protparam server. 2014. Available: URL: http://us.expasy.org/tools/protparam.html. [Last accessed 09th Apr 2014].
15. Hirokawa T, Boon-Chieng S, Mitaku S. Sosui: classification and secondary structure prediction system for membrane proteins. Bioinf 1998;14:378-79.
16. Buchan DWA, Minneci F, Nugent TCO, Bryson K, Jones DT. Scalable web services for the Psipred Protein Analysis Workbench. Nuc Acids Res 2013;41:340-8.
17. Eswar N, Marti-Renom MA, Webb B, Madhusudhan MS, Eramian D, Shen M, *et al*. Comparative protein structure modeling with modeller. Current Protocols in Bioinformatics: John Wiley & Sons, Inc; 2006. p. 15, 5.6.1-5.6.30.
18. Pettersen EF, Goddard TD, Huang CC, Couch GS, Greenblatt DM, Meng EC, *et al*. UCSF Chimera visualization system for exploratory research and analysis. J Comput Chem 2004;25:1605-12.
19. Lovell SC, Davis IW, Arendall III WB, de Bakker PIW, Word JM, Prisant MG, *et al*. Structure validation by Calpha geometry: phi, psi and Cbeta deviation. Proteins: Struct., Funct., Genet 2002;50:437-50.
20. Luthy R, Bowie JU, Eisenberg D. Assessment of protein models with three-dimensional profiles. Nat 1992;5:83-5.
21. Benkert P, Tosatto SCE, Schomburg D. Qmean: a comprehensive scoring function for model quality assessment. Proteins: Struct Funct Bioinf 2008;7:261-77.

22. Liang J, Edelsbrunner H, Woodward C. Anatomy of protein pockets and cavities: Measurement of binding site geometry and implications for ligand design. Prot Sci 1998;7:1884-97.
23. Laurie AT, Jackson RM. Q-SiteFinder: an energy-based method for the prediction of protein–ligand binding sites. Bioinf 2005;21:1908-16.
24. Pubchem project database. 2014. Available: URL: http://pubchem.ncbi.nlm.nih.gov/. [Last accessed 20th Mar 2014].
25. Chemspider database. 2014. Available: URL: http://www.chemspider.com/. [Last accessed 23rd Mar 2014].
26. Pedretti A, Villa L, Vistoli G. VEGA-An open platform to develop chemo-bio-informatics applications, using plug-in architecture and script programming. J Comput Aided Mol Des 2004;18:167-73.
27. Thompson MA. 2004. ArgusLab 4.0.1. Planaria Software LLC, Seattle, Washington. Available: URL: http://www.ArgusLab.com. [Last accessed 30th Mar 2014].
28. Schneidman-Duhovny D, Inbar Y, Nussinov R, Wolfson HJ. Patch Dock and Symm Dock: servers for rigid and symmetric docking. Nucl Acids Res 2005;33:363-7.
29. Guex N, Peitsch MC. Swiss-PdbViewer: a fast and easy-to-use PDB viewer for Macintosh and PC. Protein Data Bank Quaterly Newsletter; 1996;77:7.
30. Discovery studio visualizer 3.5. 2014. Available: URL: http://accelrys.com/products/discovery-studio/visualization-download.php. [Last accessed 25th May 2014].
31. Molegro virtual docker. 2014. Available: URL: http://molegro-virtual-docker.software.informer.com/5.5/. [Last accessed 30th May 2014].
32. Pymol. 2014. Available: URL: http://www.pymol.org/. [Last accessed 25th Apr 2014].
33. Trott O, Olson AJ. Auto Dock Vina: improving the speed and accuracy of docking with a new scoring function, efficient optimization and multithreading. J Comput Chem 2010;31:455-61.
34. Manivannan P, Ganesan S, Naveenkumar S, Daniel SD, Sathiamoorthi T, Muralitharan G. Molecular modelling of urease accessory interaction proteins of *Helicobacter Pylori* J 99 and predicting an interruption in interaction by *Vigna radiata* Defensins. Bioinf 2011;5:410-5.
35. Geetha T, Varalakshmi P. Anti-inflammatory activity of lupeol and lupeol linoleate in rats. J Ethnopharmacol 2001;76:77-80.
36. Agarwal RB, Rangari VD. Antiinflammatory and antiarthritic activities of lupeol and 19α-h lupeol isolated from *strobilanthus callosus* and *strobilanthus ixiocephala* roots. Ind J Pharmacol 2003;35:384-7.
37. Malini MM, Baskar R, Varalakshmi P. Effect of lupeol, a pentacyclictriterpene, on urinary enzymes in hyperoxaluric rats. Jpn J Med Sci Biol 1995;48:211-20.
38. Sunitha S, Nagaraj M, Varalakshmi P. Hepatoprotective effect of lupeol and lupeol linoleate on tissue antioxidant defence system in cadmium-induced hepatotoxicity in rats. Fitoterapia 2001;72:516-23.
39. Marvin JW, Yanjun Z, Muraleedharan G. Colon cancer proliferating desulphosinigrin in Wasabi (*Wasabia japonica*). Nutr Cancer 2004;48:207-13.
40. Estiu G, Merz KM. The hydrolysis of urea and the proficiency of urease. JACS 2004;126:6932-44.